

Synthesis, characterization and X-ray crystal structure of novel nickel Schiff base complexes and investigation of their catalytic activity in the electrocatalytic reduction of alkyl and aryl halides

Ali Ourari¹ · Imène Bougossa¹ · Sofiane Bouacida^{2,3} · Djouhra Aggoun¹ · Ramiro Ruiz-Rosas⁴ · Emilia Morallon⁵ · Hocine Merazig²

Received: 29 April 2016 / Accepted: 26 November 2016 / Published online: 26 December 2016
© Iranian Chemical Society 2016

Abstract Novel potentially bidentate NO Schiff base ligands, **HL**¹ and **HL**² derived from condensation reaction of 2'-methoxyphenyl-2-ethylamine with salicylaldehyde (**HL**¹) and with 2-hydroxy-4-methoxybenzaldehyde (**HL**²), and their nickel complexes were synthesized and characterized by usual spectroscopic techniques such as FT-IR, UV-Vis, ¹H NMR, ¹³C NMR and elemental analysis. It was revealed that the bidentate Schiff base ligands coordinate with Ni(II) ions yielding mononuclear complexes with 1:2 (metal/ligand) stoichiometry. This result has been determined by using X-ray crystallographic technique of **HL**² and the nickel complex derived from **HL**¹ (**Ni(II)-2L**¹). So, the structural studies showed that the two Ni(II) complexes adopt a square-planar geometry around the central metal ion. Cyclic voltammetry studies were investigated in

0.1 M TBAP in DMF solution and indicate that the nickel complexes show one reduction wave related to Ni(II)/Ni(I) redox couple. The electrocatalytic properties of these complexes were also studied in the same electrolyte medium. Their electrocatalytic performances have been tested toward the electroreduction reaction of bromocyclopentane and iodobenzene, showing a promoted activity in the case of the **Ni(II)-2L**² complex.

Keywords Bidentate Schiff base nickel(II) complexes · X-ray diffraction · Electrochemical behavior · Electrocatalytic reduction

Introduction

It has been more than a century since the Schiff bases were first reported in the seminal work of Hugo Schiff concerning the synthesis of the imino function [1, 2]. Since then, this topic has attracted the attention of most researchers working either in industry or in the universities [3–9]. These compounds were found to have good ability to coordinate transition metals through nitrogen atoms of the iminic group, which can be accompanied by other heteroatoms such as oxygen and sulfur. The chelating properties of these ligands become more and more interesting for the development of coordination chemistry, particularly with transition metals [10–14].

While the tridentates and tetradentates Schiff base ligands were involved in most studies on the topic of the coordination chemistry with transition metals [15, 16], the bidentate ligands of such kind of complexes have also been used as the modulators of structural and electronic properties of transition metal centers [17–19]. For this reason, Schiff base ligands and their metal complexes have

✉ Ali Ourari
alourari@yahoo.fr

✉ Djouhra Aggoun
aggoun81@yahoo.fr

¹ Laboratoire d'Electrochimie, d'Ingénierie Moléculaire et de Catalyse Redox (LEIMCR), Faculté de Technologie, Université Ferhat ABBAS Sétif-1, 19000 Sétif, Algeria

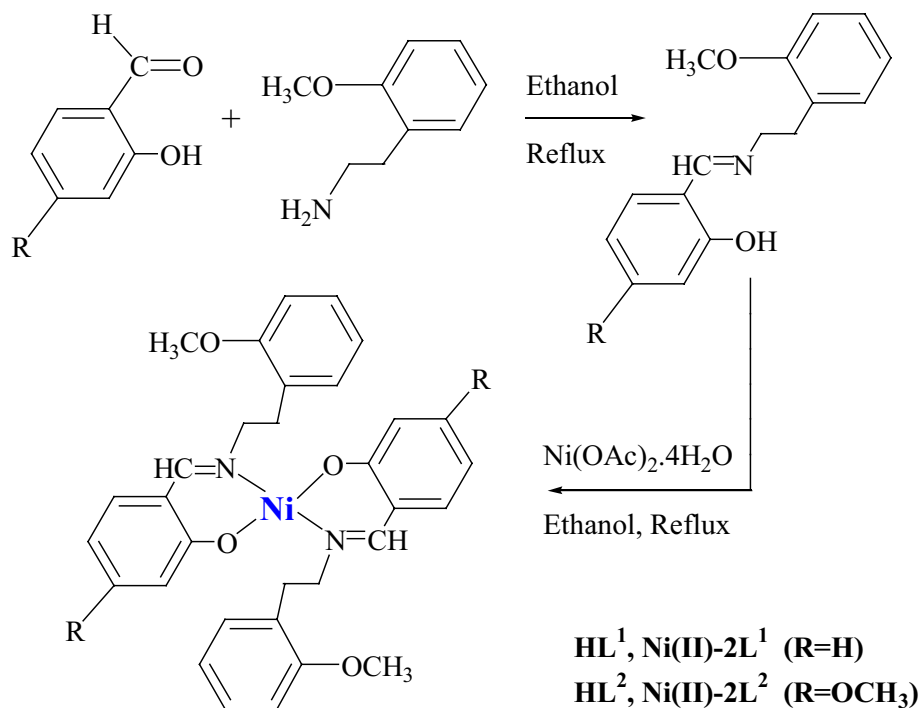
² Unité de Recherche de Chimie de l'Environnement et Moléculaire Structurale, CHEMS, Université des frères Mentouri-Constantine, 25000 Constantine, Algeria

³ Département Sciences de la Matière, Faculté des Sciences Exactes et Sciences de la Nature et de la Vie, Université Oum El Bouaghi, Oum El Bouaghi, Algeria

⁴ Departamento de Química Inorgánica, Instituto Universitario de Materiales, Universidad de Alicante, Ap. 99, 03080 Alicante, Spain

⁵ Departamento de Química Física, Instituto Universitario de Materiales, Universidad de Alicante, Ap. 99, 03080 Alicante, Spain

Scheme 1 Synthetic procedure of **HL¹**, **HL²**, **Ni(II)-2L¹** and **Ni(II)-2L²**



been found to be very useful in a wide range of applications because of the high stability of these complexes with different oxidation states. Accordingly, several of these compounds process a large amount of biological and environmental properties which could render them as very potent new probes [20]. They have been found to be highly dependent on the selectivity and sensitivity for biologically active metal ions associated with the binding sites of the ligands. As well, it seems useful to note that these compounds become more and more important as magnetic [21–23], medical imaging [24] and industrial use as catalysts [25–29].

Recently, nickel Schiff base complexes have been used as catalysts in different areas [30–33]. In this case, the electrogenerated nickel(I) Schiff base species has been used as catalysts for the reduction of organic halides using glassy carbon as cathodes in different media such as dimethylformamide (DMF), acetonitrile (AN) and dichloromethane (DC). The electrocatalytic reduction involving the reductive cleavage of carbon–halogen bonds has been well discussed in the literature [34–40] for a large variety of organic compounds.

In view of these facts, two new Schiff base ligands with their nickel(II) complexes were synthesized and characterized using different FT-IR, ¹H NMR, ¹³C NMR, UV–Vis spectroscopies and analytical methods. Crystal structures have also been determined. Electrochemical behavior of the Schiff bases and their nickel complexes was studied by cyclic voltammetry. Finally, the electrocatalytic performances of these complexes were examined in the

electroreduction reactions of two different halogenated compounds in the organic media like dimethylformamide. The synthetic procedure for the preparation of the both Schiff base ligands and their nickel complexes is shown in Scheme 1.

Experimental

Reagents and instruments

All chemicals and solvents were obtained from commercial sources and were used as received without further purification. Bromocyclopentane and iodobenzene (Aldrich, 98%) were chosen as the substrates to test the catalytic properties of the electrogenerated nickel(I) form of **Ni(II)-2L¹** and **Ni(II)-2L²**.

Purity of the synthesized compounds was checked by means of thin-layer chromatography (TLC); glass plates were precoated with silica gel (60F, Merck). Uncorrected melting points were measured with a Kofler Banc (model WME) apparatus. All new compounds were analyzed for C, H and N with the aid of a Vario EL III elemental analyzer. ¹H NMR and ¹³C NMR spectra were recorded on a 400-MHz Bruker FT-NMR spectrometer using CDCl₃ as solvent; chemical shifts (δ) are referenced to tetramethylsilane (TMS), used as internal reference and given in ppm. IR spectra were obtained as KBr plates using a Bruker FT-IR instrument. UV–Vis spectra were obtained with the aid of an UNICAM UV-300 instrument with CH₂Cl₂ solutions.

Table 1 ^1H NMR and ^{13}C NMR spectral data of the Schiff base **HL**² and complexes **Ni(II)-2L**² and **Ni(II)-2L**¹ in CDCl_3 ; a multiplicity of signals are singlet (s), triplet (t) and multiplet (m) with their chemical shifts, expressed in ppm

^1H NMR	N=CH	Ph-CH ₂ (₈)	N-CH ₂ (₉)	-OCH ₃ (₁)	-OCH ₃ (₁₇)	H _(3-6,12-13-15)
Ni(II)-2L ¹	8.90 (s, 1H)	3.20 (t, 2H)	4.09 (t, 2H)	3.82 (s, 3H)	–	5.80–7.50 (m, 8H)
HL ²	7.94 (s, 1H)	3.73 (t, 2H)	2.99 (t, 2H)	3.79 (s, 3H)	3.82 (s, 3H)	7.27–6.80 (m, 7H)
Ni(II)-2L ²	10.2 (s, 1H)	3.20 (t, 2H)	4.60 (t, 2H)	3.70 (s, 3H)	3.90 (s, 3H)	5.80–7.50 (m, 7H)
^{13}C NMR	N=C ₍₁₀₎ H	N-CH ₂ (₉)	Ph-CH ₂ (₈)	-OCH ₃ (₁)	-OCH ₃ (₁₇)	C _(2-7, 11-16)
Ni(II)-2L ¹	163.90	58.24	43.40	55.10	–	110–160
HL ²	168.29	56.81	32.26	55.33	55.40	100–140
Ni(II)-2L ²	164.09	58.78	35.05	55.16	55.44	100–140

The cyclic voltammograms were recorded using a 10-ml three-electrode cell in DMF solutions containing 0.1 M tetra-*n*-butylammonium perchlorate (TBAP). The electrodes were polished by diamond paste and rinsed with acetone and DMF. Working electrode was a disc of glassy carbon (diameter 3 mm), while the counter electrode was a platinum wire, and the reference was a saturated calomel electrode (SCE). Zero-grade argon (air products) was used to deaerate all solutions.

X-ray crystallography

Prismatic colorless single crystals of **HL**² and green single crystals of **Ni(II)-2L**¹ were obtained by slow evaporation from dichloromethane solution. The crystal was coated with paratone oil and mounted on loops for data collection. X-ray data were collected with a Bruker Apex II CCD area detector diffractometer with a graphite-monochromated Mo-K α radiation source (0.71073 Å) at 298 K. The reported structure was solved by direct methods with SIR2002 [41] to locate all the non-H atoms which were refined anisotropically with SHELXL97 [42] using full-matrix least squares on F² procedure from within the WinGX [43] suite of software used to prepare material for publication. All the H atoms were placed in the calculated positions and constrained to ride on their parent atoms. Drawings of molecules were produced with the program ORTEP-3 [44]. Crystal data and refinement results are given in Table 1.

General procedure for the synthesis

Synthesis of **HL**¹ and **Ni(II)-2L**¹

2-Methoxyphenylethylamine (1 mmol, 151.21 mg) and 2-hydroxybenzaldehyde (1 mmol, 122 mg) were dissolved in absolute ethanol (16 ml). The mixture was refluxed for 3 h to prepare the Schiff base ligand (**HL**¹). The yellow resulting oil was cooled without isolating. An ethanol

solution of $\text{Ni}(\text{OCOCH}_3)_2 \cdot 4\text{H}_2\text{O}$ (0.5 mmol, 124.42 mg) was added to it and refluxed again for additional 4 h. A green solid was recovered and collected by filtration and washed with small portions of cooled ethanol. Single crystals, suitable for X-ray diffraction, were obtained from dichloromethane solution of the complex with slow evaporation in an open atmosphere.

Yield 170 mg (30%). Color (Green). M.p. = 163 °C. **IR** (*KBr*, cm^{-1}): 1608 (HC=N), 2955 and 2900 (CH_{aliph}), 1240 (C–O), 580–660 (Ni–O), 400–480 (Ni–N). **^1H NMR** (*DMSO-d*₆, δ , ppm): 5.80–7.50 (m, 8H, Ar–H), 8.90 (s, 1H, N=CH), 4.09 (t, 2H, N–CH₂), 3.82 (s, 6H, methoxy –OCH₃), 3.2 (t, 2H, Ph–CH₂). **Anal. Found for $\text{C}_{32}\text{H}_{31}\text{N}_2\text{NiO}_4$** (566.3 g mol^{–1}): C: 68.18; H: 5.75; N: 5.09; Calc.: C: 67.87; H: 5.52; N: 4.95%.

Synthesis of **HL**² and **Ni(II)-2L**²

2-Methoxyphenylethylamine (1 mmol, 151.21 mg) and 2-hydroxy-4-methoxybenzaldehyde (1 mmol, 152.15 mg) were dissolved in absolute ethanol (16 ml). The mixture was refluxed for 3 h. The resulting yellow solution was left to stand at room temperature in an open atmosphere. **HL**² was obtained as single crystals. These single crystals were analyzed by X-ray diffraction.

Yield 60 (%). Color (Yellow). M.p. = 58 °C. **IR** (*KBr*, cm^{-1}): 3320–3640 (–OH), 1610 (HC=N), 2935 and 2825 (CH_{aliph}), 1248 (C–O). **^1H NMR** (*DMSO-d*₆, δ , ppm): 6.80–7.27 (m, 7H, Ar–H), 7.94 (s, 1H, N=CH), 2.99 (t, 2H, N–CH₂), 3.79 (s, 6H, methoxy –OCH₃), 3.73 (t, 2H, Ph–CH₂). **Anal. Found for $\text{C}_{17}\text{H}_{19}\text{O}_3\text{N}$. 0.5 H_2O** (294.345 g mol^{–1}): C: 69.55; H: 7.02; N: 4.89; Calc.: C: 69.37; H: 6.85; N: 4.76%.

A 8-ml ethanolic solution of $\text{Ni}(\text{OCOCH}_3)_2 \cdot 4\text{H}_2\text{O}$ (124.4 mg, 0.5 mmol) was prepared and added to 8 ml

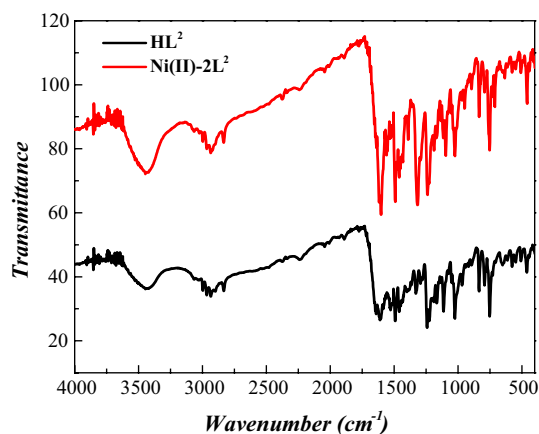


Fig. 1 IR spectra of the **HL**² and its nickel complex

ethanolic solution of the **HL2** (285 mg, 1 mmol). A green precipitate was immediately observed, and then, the mixture was refluxed for 4 h. The reaction mixture was cooled to room temperature, and the solid was then recovered by filtration, washed with small portions of cooled ethanol, dried and weighted.

Yield 256 mg (40%). Color (Green). M.p. = 199 °C. **IR** (*KBr*, cm^{-1}): 1598 (HC=N), 2935 and 2825 (CH_{aliph}), 1233 (C–O), 500–650 (Ni–O), 420–480 (Ni–N). **¹H NMR** (*DMSO-*d*₆*, δ , ppm): 5.80–7.50 (m, 7H, Ar–H), 10.2 (s, 1H, N=CH), 4.60 (t, 2H, N–CH₂), 3.70 (s, 6H, methoxy –OCH₃), 3.20 (t, 2H, Ph–CH₂). **Anal. Found for C₃₄H₃₆O₆N₂Ni** (627.35 g mol^{−1}): C: 65.12; H: 5.80; N: 4.13; Calc.: C: 65.09; H: 5.78; N: 4.47%.

Results and discussion

Physicochemical properties of the synthesized compounds

The ligand and the both complexes of nickel were found to be stable at room temperature, and they could be dissolved in DMF, DMSO, ACN and dichloromethane. The evidence for the formation of the Schiff base ligand (**HL**¹ and **HL**²) was confirmed by using various spectral techniques. Elemental analysis and analytical data agree well with the proposed structure of Schiff base ligand (**HL**²) and the two nickel Schiff base complexes (**Ni(II)-2L**¹ and **Ni(II)-2L**²). These data of metal complexes suggest that the metal/ligand molecular ratio for the complexes is 1:2.

IR spectral studies

In IR spectrum (Fig. 1), the bidentate Schiff base ligand (**HL**²) exhibits a broad absorption band centered around 3446 cm^{-1} that can be assigned to O–H stretching arising from the presence of hydroxyl group. The hydrocarbon part of this ligand was evidenced by the presence of unsymmetrical and symmetrical frequencies of ν_{CH_2} observed at 2935 and 2825, respectively. The presence of an intense band in the spectrum of **HL**² at $\nu_{\text{HC=N}}$ 1610 cm^{-1} was assigned to the stretching vibration of the azomethine group. This band is also present in the IR spectrum of the **Ni(II)-2L**² complex (see Fig. 1), but, in this case, it has been shifted to lower wave numbers and appears at around $\nu_{\text{HC=N}}$ 1598 cm^{-1} , suggesting that the metallic ion was effectively coordinated to the four coordinating heteroatoms (**NONO**). Therefore, this is in good agreement with an important extension of electronic delocalization [45]. The band located at 1248 cm^{-1} for the ligand **HL**² is ascribed to the phenolic C–O stretching vibration. This band is shifted to the lower frequencies (1233 cm^{-1}) due to oxygen–nickel coordination. Another conclusive evidence for the formation of Ni–N and Ni–O bonds in the IR spectrum of this complex (**Ni(II)-2L**²) is also shown by the appearance of new bands at around 420–480 and 500–650 cm^{-1} . These absorption bands were attributed to the Ni–N and Ni–O stretching vibrations, respectively [46].

As for the IR spectrum of the complex **Ni(II)-2L**¹, it shows also an intense band at around 1608 cm^{-1} which is assignable to the stretching vibration of the azomethine groups. In addition, the spectrum exhibits strong vibration at 1240 cm^{-1} which is assigned to stretching of C_{aromatic}–O–C_{aliphatic} group. Stretching vibrations of Ni–N in the complex are seen as weak absorption frequencies at 400–480 cm^{-1} that confirm the coordination of two azomethine nitrogen atoms of Schiff base ligands. Finally, the appearance of other bands at around 580 and 660 cm^{-1} was ascribed to the Ni–O stretching vibrations [46].

UV–Vis spectral studies

The UV–Vis spectrum of the ligand **HL**² (Fig. 2a) shows two intense bands at 302 ($\epsilon = 1.890.105 \text{ mol}^{-1} \text{ L cm}^{-1}$) and 387 nm ($\epsilon = 0.325.105 \text{ mol}^{-1} \text{ L cm}^{-1}$), and these bands may be assigned to $n\text{--}\pi^*$ transition [47, 48]. Substitution in the aromatic ring of the ligand results a bathochromic shift, which is strongest for methoxy group, since it has the most activating influence on ligands containing substituted aromatic rings [49]. These peaks are partially present in the electronic absorption spectra of the complex **Ni(II)-2L**² and are different in the **Ni(II)-2L**¹ complex.

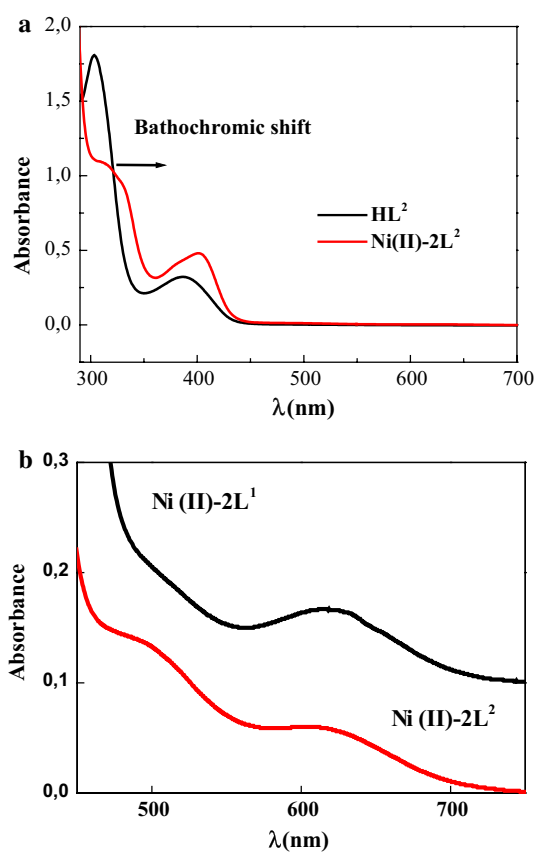


Fig. 2 UV-Vis spectra of the 10^{-5} M CH_2Cl_2 solutions of the HL^2 and Ni(II)-2L^2 complex (a). The inset shows the MLCT and d-d transition region with 10^{-3} M solutions (b) of the both complexes

The shifting of the band ($n \rightarrow \pi^*$ transitions of the $\text{C}=\text{N}$ groups) in Ni(II)-2L^2 is also indicative of the coordination of the nitrogen atom of the azomethine groups to the metal center. The electronic absorption spectra of the complexes show a shoulder at 498 nm which is assigned to the MLCT expressing the charge transfer between the metallic center and the coordinating atoms of the ligands [50]. The weak bands observed at about 616 nm ($\epsilon = 0.167 \cdot 10^3 \text{ mol}^{-1} \text{ L cm}^{-1}$) for Ni(II)-2L^1 and 600 nm ($\epsilon = 0.059 \cdot 10^3 \text{ mol}^{-1} \text{ L cm}^{-1}$) for Ni(II)-2L^2 are attributable to the d-d transitions [51] (see Fig. 2b).

^1H NMR and ^{13}C NMR spectra

The ^1H NMR and ^{13}C NMR spectral data of the Schiff base HL^2 , Ni(II)-2L^2 and Ni(II)-2L^1 complexes are listed in Table 1. The ^1H NMR spectrum of the Schiff base ligand HL^2 (see Fig. 3) shows a sharp singlet signal (s) at 7.94 ppm attributed to the azomethine proton ($-\text{HC}=\text{N}-$). The methylene group $\delta \text{ Ph-CH}_2(8)$ resonates at 3.73 ppm. As for the $\text{N-CH}_2(9)$, it absorbs at 2.99 ppm.

The deshielding effects of the phenyl and azomethine groups may be estimated from the difference of chemical shifts $\delta \text{ N-CH}_2(9)$ (3.73 ppm) and $\delta \text{ Ph-CH}_2(8)$ (2.99 ppm) leading to the delta value equal to 0.74 ppm. This difference expresses that the aromatic entity exhibits a higher deshielding effect when compared to the azomethine group with its unique double bond. The protons of the both methoxy groups appear as different resonating with two different chemical shifts such as $\delta \text{CH}_3\text{O}$ of the complex which were observed at 3.79, while those of its Schiff base ligand (HL^2) were resonated at 3.82 ppm. In this case, the difference between the two (δ) chemical shifts for the methoxy protons seems to be slightly weaker, since it equals only to 0.03 ppm. This difference may be attributed to the extension of the electronic delocalization, caused by the nickel ion coordinating the both salicylaldehyde entities. For the second methoxy, grafted to the aminic group, its protons share the same previous electronic effect with another ethylene group ($-\text{CH}_2-\text{CH}_2-$) leading to the minimization of the same deshielding effect, giving only 3.79 ppm. A multiplet was observed for the ligand between 6.80 and 7.27 ppm; thus, its chemical shift is located at 7.00 ppm. Concerning the same protons belonging to both complexes Ni(II)-2L^1 and Ni(II)-2L^2 , their multiplets were observed in the range 5.80–7.50 ppm. They were noted at 6.85 and 6.65 ppm, respectively.

As for the ^{13}C NMR spectra, the HL^2 Schiff base ligand shows the azomethine carbon peak at 168.29 ppm. The aliphatic $\text{Ph-CH}_2(8)$, $\text{N-CH}_2(9)$, $-\text{OCH}_3(1)$ and $-\text{OCH}_3(17)$ carbon peaks are detected at 32.26, 56.81, 55.33 and 55.40 ppm, respectively (Fig. 3). The aromatics carbons are observed in the expected region between 127 and 133 ppm. In the ^{13}C NMR spectra of the complexes, all the carbons peaks are slightly shifted upfield and downfield.

Description of crystal structures

ORTEP representations of HL^2 and Ni(II)-2L^1 (CCDCs: 1495692 and 1495691, respectively) are shown in Figs. 4 and 5, respectively. Crystallographic data and structure refinement parameters are given in Table 2, and selected bond distances and angles are given in Table 3.

The ligand HL^2 (Fig. 4) crystallizes in the monoclinic space group $P 2_1/c$ with 2 formula units in the cell. The azomethine connection is evident from the N1-C10 bond length (1.290 Å) and C10-N1-C9 angle (121.4°). The bond length and angle around the azomethine group are in agreement with sp^2 hybridization of its carbon atom. As for the Ni(II)-2L^1 (Fig. 5), this complex crystallizes in the orthorhombic space group $\text{Pca}2_1$ with 4 formula units in the cell. The crystal structure of Ni(II)-2L^1 shows a tetradentate NONO coordination of the two bidentate Schiff base ligands. The nickel ion is situated in a square-planar

Fig. 3 ^1H NMR and ^{13}C NMR spectra of the Schiff base HL^2 and its nickel complex

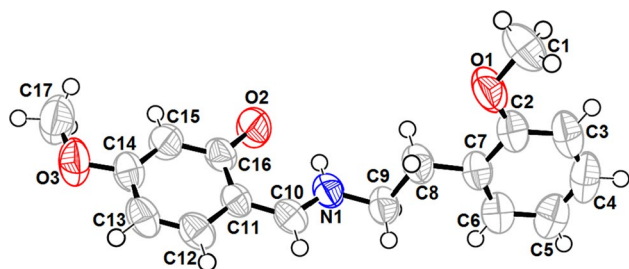
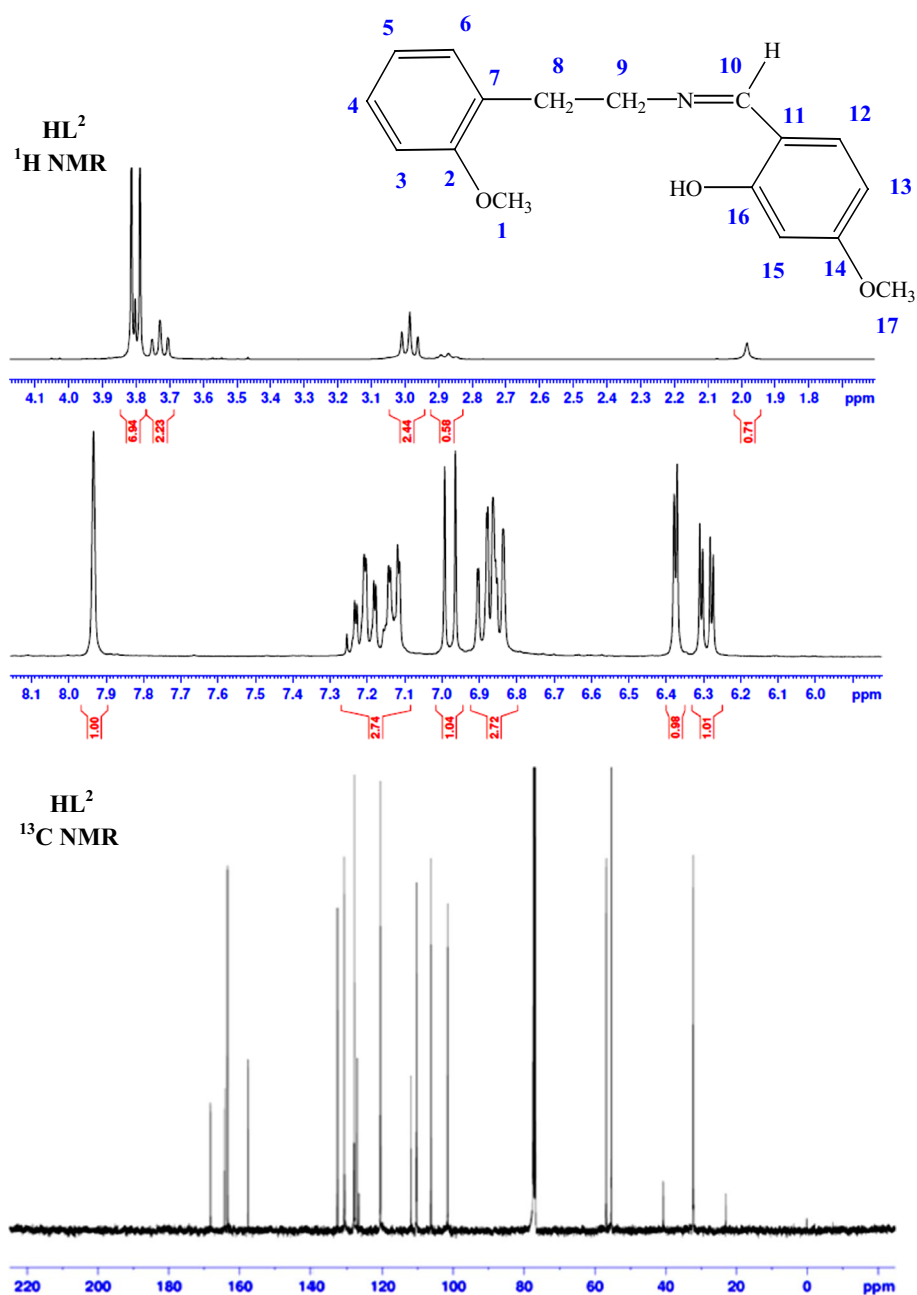


Fig. 4 ORTEP representation of HL^2 . Displacement ellipsoids are drawn at the 50% probability level, and H atoms are shown as *small spheres* of arbitrary radii

environment, coordinated in the *trans* position by two oxygen atoms of the ligand. This coordination environment is satisfied by the phenoxo oxygen and imine nitrogen atoms of the Schiff base ligand [Ni: O1, O2, N1, N2]. The azomethine linkage is evident from the N1–C20 and N2–C7 bond lengths (1.289 and 1.289 Å, respectively), C20–N1–C21 and C7–N2–C9 angles (113.7° and 114.1°, respectively). The bond lengths involving the phenyl carbon and phenoxo oxygen atoms, C1–O1, C18–O2, C16–O3 and C27–O4, are 1.298, 1.301, 1.383 and 1.372 Å, respectively, and these values are in the range of the usually observed standard $\text{C}(sp^2)\text{--OH}$ and $\text{C}(sp^2)\text{--O}$ – bond length. The Ni–O and

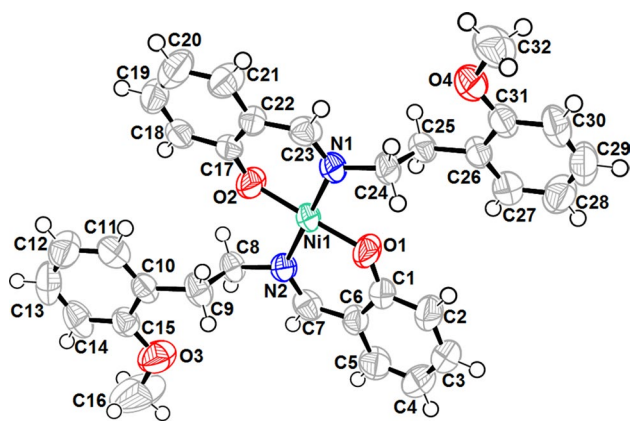


Fig. 5 ORTEP representation of the centrosymmetric complex **Ni(II)-2L¹**. Displacement ellipsoids are drawn at the 50% probability level, and H atoms are shown as *small spheres* of arbitrary radii

Ni–N bond lengths for **Ni(II)-2L¹** varying in the range 1.821–1.831 Å and 1.918–1.919 Å, respectively, are in good agreement with related reported complexes. Cisoid and transoid angles of the nickel deviate from their ideal values of 90° and 180° and found to be in the ranges 86.3°–93.1° and 178.2°–176.5°, respectively. The bond lengths and angles around C17 and C28 (methoxy atoms) are in agreement with *sp³* hybridizations of this atom.

Electrochemistry

The electrochemical behavior of the **HL¹** and **HL²** ligands and the corresponding nickel complexes (**Ni(II)-2L²** and **Ni(II)-2L¹**) was studied at 25 °C using dimethylformamide solutions (DMF) with 0.1 M tetra-*n*-butylammonium perchlorate (TBAP) as supporting electrolyte at a glassy carbon working electrode under an argon atmosphere. The approximate concentrations of the compounds were 10^{−3} M.

Cyclic voltammetry of the ligands

It is evident from the cyclic voltammogram of **HL¹**, displayed in Fig. 6, that the ligand is electroactive over a range from +1.8 to −2.5 V in DMF solvent using a scan rate of 100 mV s^{−1}. The voltammogram shows two oxidation waves: The first is observed at $E_{pa1} = 0.19$ and may be ascribed to the oxidation of the methoxy group, while the second one is observed at $E_{pa2} = 1.385$ V/SCE and may be assigned to the oxidation of the phenolic function. Concerning the reductions sweep, also two reduction waves are observed at $E_{pc1} = -1.074$ and $E_{pc2} = -2.050$ V/SCE, respectively. The first is attributed to the reduction of the

oxidized methoxy function, while the last wave seems to be an irreversible system and may be ascribed to the electrochemically reduction of azomethine function. The same results were observed in the cyclic voltammogram of the second ligand **HL²**.

Cyclic voltammetry of the Ni(II)-2L¹ and Ni(II)-2L²

Cyclic voltammetry of the complexes **Ni(II)-2L¹** and **Ni(II)-2L²** was performed in the potential range of −2.0 to 1.6 V/SCE and −2.2 to 1.6 V/SCE, respectively.

In the case of the **Ni(II)-2L¹** complex, the cyclic voltammogram presented in Fig. 7 shows four oxidation waves located at $E_{pa1} = -1.465$, $E_{pa2} = 0.807$, $E_{pa3} = 0.976$ V/SCE and $E_{pa4} = 1.205$ V/SCE, respectively. The first and the second ones are ascribed to the Ni (I)/Ni (II) and Ni (II)/Ni (III) oxidation reactions, while the third and the last one may be assigned to the oxidation of the bidentate Schiff base ligand. Concerning the reduction sweep, two reduction waves can be observed at $E_{pc1} = 0.685$ and $E_{pc2} = -1.54$ V/SCE: The first is of the Ni (III)/Ni (II) species and the second one for the reduction of Ni (II)/Ni (I) couple.

The cyclic voltammogram of the second complex of nickel (**Ni(II)-2L²**) exposed clearly the same comportment with three redox systems. Initially, an irreversible wave in the range +0.2 to +0.8 V is observed, due to the electrochemically irreversible Ni (III)/Ni (II) reductive response. Then, the second system is attributed to the Ni (II)/Ni (I) system and its $\Delta E_p = (E_{pa} - E_{pc})$ value was estimated to be 140 mV, while the last system situated between −2.2 and −1.8 V/ECS seems to be also an irreversible system and may be ascribed to the reduction of imino function.

As a conclusion, in the voltammograms of the both complexes (see Fig. 7), the quasi-reversible redox processes were noticed and correspond to a monoelectronic transfer for the both complexes **Ni(II)-2L¹** and **Ni(II)-2L²**. The redox species involved in these processes are the well-known Ni (II)/Ni (I) couple. It is also important to note that the Ni (III)/Ni (II) redox systems habitually observed in anodic side cannot be clearly seen on the voltammograms. This electrochemical behavior has been already observed for Ni–ligand complexes [52, 53].

Electrochemical reduction of bromocyclopentane and iodobenzene using Ni(II)-2L¹ and Ni(II)-2L² as electrocatalysts

The nickel complexes were found to be efficient for the electrocatalytic reduction of alkyl and aryl halides compounds such as bromocyclopentane and iodobenzene in

Table 2 Crystal data, data collection and structure refinement parameters for **HL²** and **Ni(II)-2L¹**

	HL²	Ni(II)-2L¹
Empirical formula	C ₁₇ H ₁₉ N O ₃	C ₃₂ H ₃₁ N ₂ Ni O ₄
Formula weight	285.33	566.28
<i>T</i> (K)	295	295
λ (Å)	0.71073	0.71073
Crystal system	Monoclinic	Orthorhombic
Space group	P 2 ₁ /c	Pca2 ₁
Unit cell dimensions (Å, °)		
<i>a</i> (Å)	5.6249 (8)	22.439 (8)
<i>b</i> (Å)	13.5439 (16)	14.690 (5)
<i>c</i> (Å)	19.730 (2)	8.322 (3)
(°) α	90	90
(°) β	90.81	90
(°) γ	90	90
Volume (Å ³), <i>Z</i>	1502.9 (3), 4	2743.2 (16), 4
Calculated density (g cm ⁻³)	1.261	1.371
Absorption coefficient (mm ⁻¹)	0.086	0.748
<i>F</i> (000)	608.0	1188
θ range for data collection (°)	3.01–26.39	2.7–30.6
Limiting indices	<i>h</i> : –7/6 <i>k</i> : –16/12 <i>l</i> : –19/24	<i>h</i> : –31/25 <i>k</i> : –10/21 <i>l</i> : –11/7
Data/restraints/	3053/0/	6910/1/
Parameters	192	354
Total reflections	11842	17815
Unique reflections (<i>R</i> _{int})	3053 (0.057)	6910 (0.0392)
Completeness	0.996	0.975
Refinement method	Full least-squared (Shelxl)	Full least-squared (Shelxl)
Goodness of fit on <i>F</i> ²	0.959	0.975
Final <i>R</i> index [<i>I</i> > 2 σ (<i>I</i>)]	0.0527	0.0444
<i>R</i> index [all data]	0.1438	0.0896
Largest difference peak and hole (<i>e</i> Å ⁻³)	0.148/–0.161	0.633/–0.27

$$R = \{\sum[w(|F_o| - |F_c|)]/\sum w(|F_o|)\}, \quad R_w = \{\sum[w(|F_o| - |F_c|)^2]/\sum w(|F_o|^2)\}^{1/2}$$

$$wR2 = \left\{ \sum \left[w(F_o^2 - F_c^2)^2 \right] / \sum w(F_o^2) \right\}^{1/2}$$

$$w = 1/[\sigma^2(F_o^2) + (0.0794P)^2 + 0.6853P] \quad \text{where } P = (F_o^2 + 2F_c^2)/3$$

Table 3 Selected bond lengths and angles for **HL²** and **Ni(II)-2L¹**

Compounds	Bond	<i>d</i> (Å)	Angle	Ω (°)	Angle	Ω (°)
HL²	C9–N1	1.452	C1–O1–C2	118.1	C11–C16–O2	120.1
	C10–N1	1.290	C7–C2–O1	114.3	C15–C16–O2	121.6
	C14–O3	1.368	C3–C2–O1	124.2	C13–C14–O3	120.4
	C16–O2	1.287	C8–C9–N1	110.3	C15–C14–O3	124.9
	C17–O3	1.424	C11–C10–N1	124.3	C14–O3–C17	117.9
			C10–N1–C9	121.4		
Ni(II)-2L¹	Ni(1)–O(1)	1.831	O2–Ni1–O1	178.2	O1–Ni1–N2	92.7
	Ni(1)–O(2)	1.821	O2–Ni1–N1	93.1	O2–Ni1–O1	176.5
	Ni(1)–N(1)	1.918	O2–Ni1–N2	86.3		
	Ni(1)–N(2)	1.919	O1–Ni1–N1	87.8		

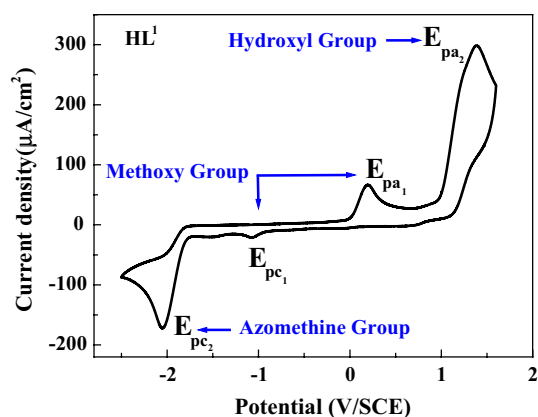


Fig. 6 Cyclic voltammogram of the HL^1 ligand in DMF at 298 K, $c = 1.10^{-3}$ M, scan rate = 100 mV s^{-1}

homogeneous phase. So, Fig. 8 shows the voltammograms obtained with Ni(II)-2L^1 and Ni(II)-2L^2 solution in the presence of bromocyclopentane. The electrocatalytic behavior of the electrogenerated Ni(I)-2L^1 (a) and Ni(I)-2L^2 (b) species is evident with scanning to the lower potential values. When an equimolar amount of bromocyclopentane with respect to the total number of nickel centers is added to a Ni(II)-2L^1 and Ni(II)-2L^2 solutions (curves B in a and b), the CV shows the increases in the reduction current associated with the bromocyclopentane (seen as negative shift on intensity from curves A to curves B) at potentials under -1.4 V. This reduction current increases with the concentration of bromocyclopentane. The cathodic peak current for the reduction of Ni(II)-2L^1 and Ni(II)-2L^2 also increases, while the anodic peak currents expressing the re-oxidation of Ni(I)-2L^1 and Ni(I)-2L^2 species disappear, indicating that all catalytic sites (metallic centers) are involved in the chemical reaction. It should be noted that Ni(I)-2L^2 complex shows the better catalytic activity, as pointed out by the higher reduction current, reached in the presence of bromocyclopentane (Fig. 8b). An increase in the concentration of bromocyclopentane causes for both complexes a significant enhancement of the cathodic peak current (curves B and C in a and b) that is not proportional to the substrate concentration. Thus, this behavior is assigned to sluggish regeneration of Ni(II)-2L^1 and Ni(II)-2L^2 species [54, 55]. The effect of the scan rate in the current density is analyzed in Fig. 8, where cyclic voltammograms recorded at different scan rates in 1.0 mM solution of Ni(I)-2L^1 (c) and Ni(I)-2L^2 (d) containing 4.0 mM of bromocyclopentane are shown. The inset shows the plot of cathodic peak current (I_{pc}) versus the square root of scan rate ($v^{1/2}$ (v is the scan rate)).

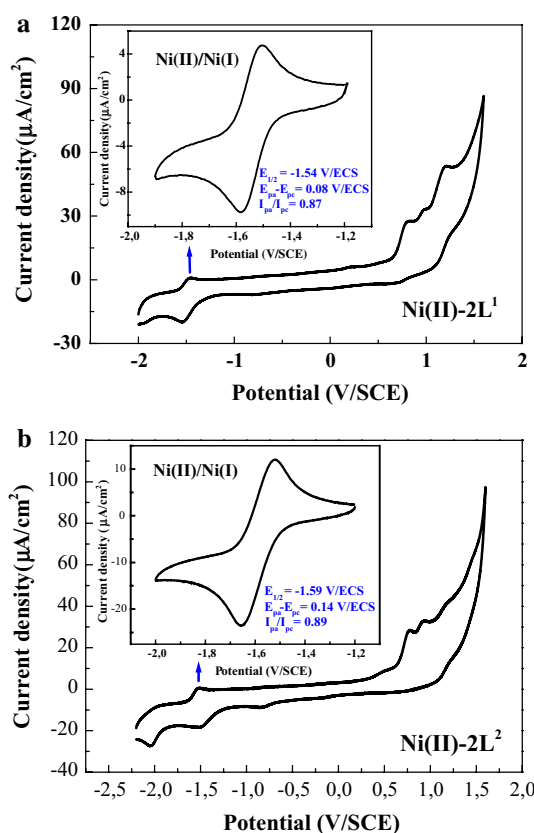


Fig. 7 Cyclic voltammograms of complexes of Ni(II)-2L^1 (a) and Ni(II)-2L^2 (b) with Ni(II)/Ni(I) redox couples, recorded in 0.1 mol L^{-1} TBAP/DMF solution at 298 K and scan rate of 100 mVs^{-1}

This plot gives a high degree of linearity, which explains the occurrence of a reversible redox process under diffusional control.

Figure 9 shows the voltammograms obtained in the presence of iodobenzene and 1 mM Ni(I)-2L^1 (a) and Ni(I)-2L^2 (b) solutions in DMF/TBAP 0.1 M. In this case, also an electrocatalytic behavior is observed in the reduction of iodobenzene. Again, when an equimolar amount of iodobenzene is added to the Ni(II)-2L^1 and Ni(II)-2L^2 solutions (curves B in a and b), the CV features of Ni(II)-2L^1 and Ni(II)-2L^2 change significantly, with the latter ligand producing a better electrocatalytic activity (as expressed by the higher current density of the reduction peak) than the former one. Figure 9 shows also the cyclic voltammograms of a 1.0-mM solution of Ni(I)-2L^1 (c) and Ni(I)-2L^2 (d) at different scan rates, containing 4.0 mM of iodobenzene. Similar features to that obtained for bromocyclopentane are seen in the plot of I_{pc} versus $v^{1/2}$ for iodobenzene (inset of Fig. 9), giving a high degree of linearity.

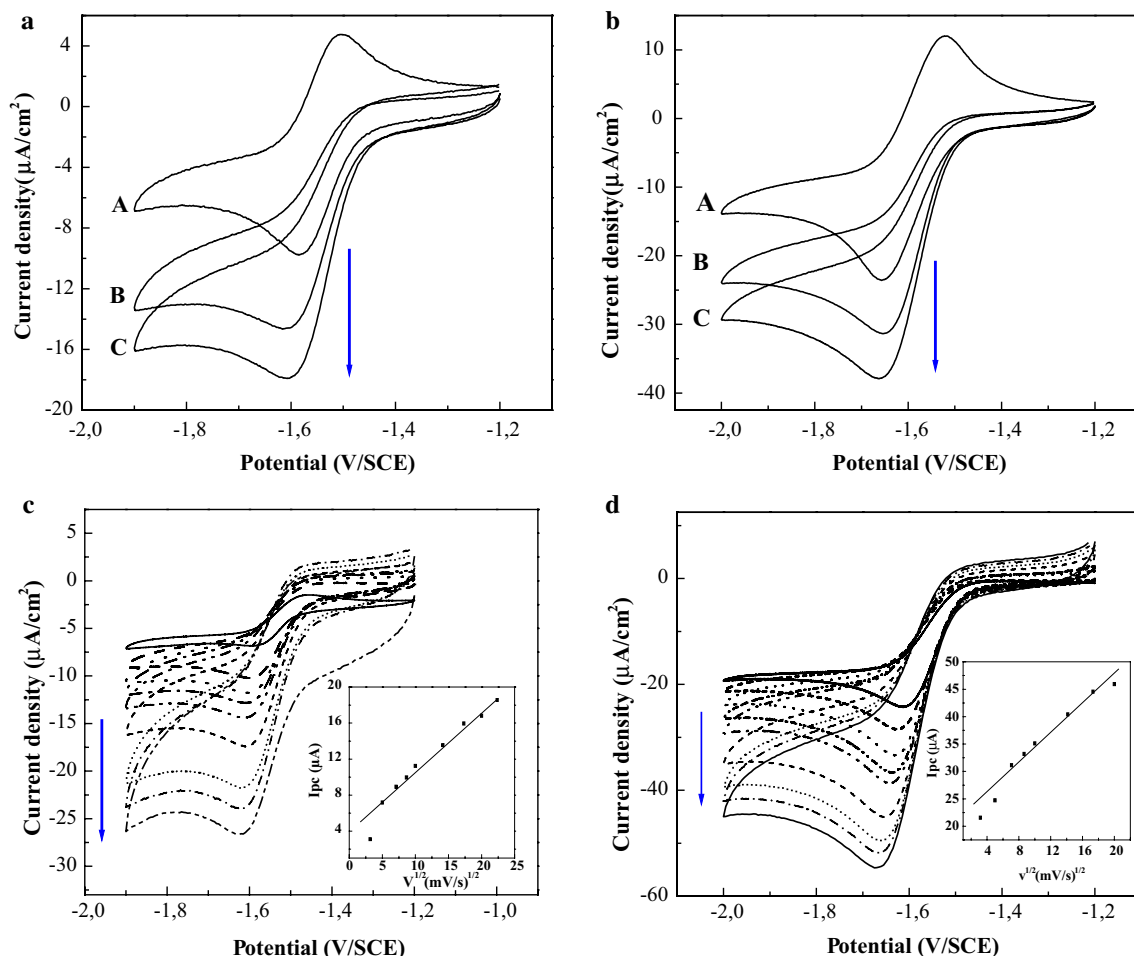


Fig. 8 Cyclic voltammograms for reduction of a 1.0-mM solution of **Ni(II)-2L¹**(a) and **Ni(II)-2L²**(b) with a glassy carbon electrode in (DMF/TBAP, 0.1 M) at a scan rate of 100 mV s⁻¹ containing (A) 0 mM; (B) 2.0 mM; (C) 4.0 mM of bromocyclopentane; CV of a 1.0-

mM solution of **Ni(II)-2L¹** (c) and **Ni(II)-2L²** (d) at different scan rates (10, 25, 50, 75, 100, 200, 300, 400, 500 mV s⁻¹) containing 4.0 mM of bromocyclopentane with the plot of cathodic peak current versus the square root of scan rate

Conclusion

In this work, we have presented the synthesis of two new nickel(II)-Schiff base complexes with their corresponding bidentate Schiff base ligands. These compounds have been then characterized by spectroscopic techniques such as IR, UV–Vis, ¹H and ¹³C NMR spectroscopy and elemental analysis, while single crystals were also obtained and analyzed by XRD. All these measures confirm the molecular structures of the both complexes. All these measures allowed us to confirm the molecular structures of the both complexes. The electrochemical behavior of our compounds has also been investigated, while the electrocatalytic properties of these complexes have as well tested for the reduction of two organic halides. It was revealed that both nickel complexes such as **Ni(II)-2L¹** and **Ni(II)-2L²**

were electrocatalytically active toward the electroreduction of bromocyclopentane and iodobenzene. The mechanistic process, involved in this electroreduction reaction, is probably produced by the corresponding electrogenerated nickel(I) species. These results have shown that the **2L²** ligands induce a higher electrocatalytic reduction activity for **nickel(I)**.

Supplementary data

Crystallographic data have been deposited at the Cambridge Crystallographic Data Centre. CCDCs 1495692 and 1495691 contain the supplementary crystallographic data for **HL²** and **Ni(II)-2L¹**. These data can be obtained free of charge via <http://www.ccdc.cam.ac.uk/conts/retrieving>.

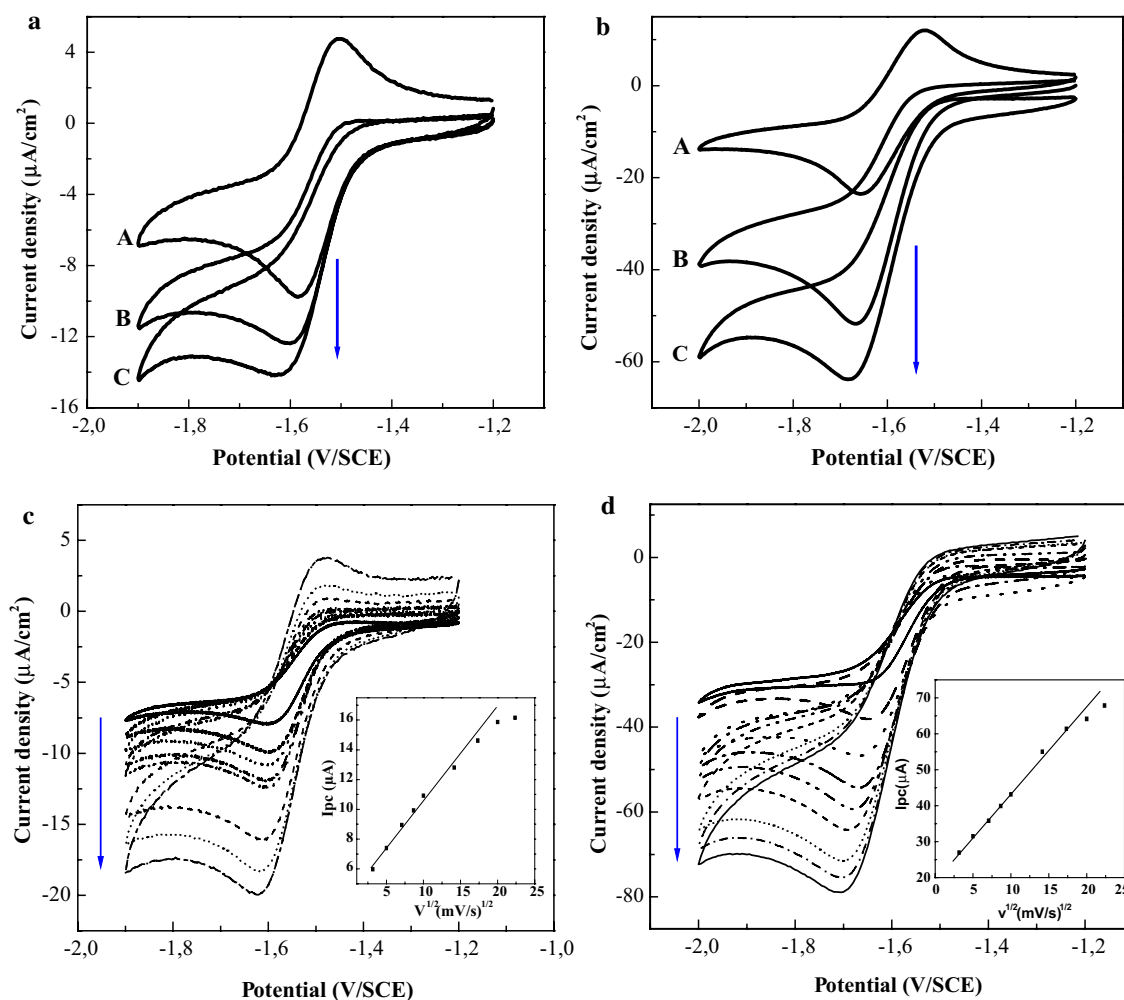


Fig. 9 Cyclic voltammograms for reduction of a 1.0-mM solution of Ni(I)-2L^1 (a) and Ni(I)-2L^2 (b) with a glassy carbon electrode in (DMF/TBAP, 0.1 M) at a scan rate of 100 mV s^{-1} , containing (A) 0 mM; (B) 2.0 mM; (C) 4.0 mM of iodobenzene; CVs of a 1.0-mM

solution of Ni(I)-2L^1 (c) and Ni(I)-2L^2 (d) at different scan rates (10, 25, 50, 75, 100, 200, 300, 400, 500 mV s^{-1}) containing 4.0 mM of iodobenzene with the plot of cathodic peak current versus the square root of scan rate

html, or from the CCDC, 12 Union Road, Cambridge, CB2 1EZ, UK; fax: (+44) 01223-336-033; e-mail: deposit@ccdc.cam.ac.

Acknowledgements The authors would like to thank the Algerian Ministère de l'Enseignement Supérieur et de la Recherche Scientifique et la Direction générale de la Recherche and Ministerio de Economía y Competitividad for financial support (MAT2013-42007-P). RUIZ-ROSAS Ramiro thanks Spanish Ministry of Economy and Competitiveness (MINECO) for a "Juan de la Cierva" contract (JCI-2012-12664).

References

- H. Schiff, Untersuchungen über Salicinderivate. *Ann. Chem.* **150**, 193–200 (1869)
- H. Schiff, Ueber condensirte Harnstoffe. *Ann. Chem.* **151**, 186–213 (1869)
- R.H. Holms, Studies on Ni(II) complexes. I. Spectra of tricyclic schiff base complexes of Cu(II) and Ni(II). *J. Am. Chem. Soc.* **82**, 5632–5636 (1960)
- E.C. Niederhoffer, J.H. Timmons, A.E. Martell, Thermodynamics of oxygen binding in natural and synthetic dioxygen complexes. *Chem. Rev.* **84**, 137–203 (1984)
- K. Srinivasan, P. Michaud, J.K. Kochi, Epoxidation of olefins with cationic (salen) manganese(III) complexes. The modulation of catalytic activity by substituents. *J. Am. Chem. Soc.* **108**, 2309–2320 (1986)
- W. Zhang, J.L. Loebach, S.R. Wilson, E.N. Jacobsen, Enantioselective epoxidation of unfunctionalized olefins catalyzed by (salen)manganese complexes. *J. Am. Chem. Soc.* **112**, 2801–2803 (1990)
- J. Tisato, F. Refosco, F. Bandoli, Structural survey of technetium complexes. *Coord. Chem. Rev.* **135**(136), 325–397 (1994)
- P.J. Lacroix, Second-order optical nonlinearities in coordination chemistry: the case of bis(salicylaldiminato)metal Schiff base complexes. *Eur. J. Inorg. Chem.* **2001**, 339–348 (2001)
- J. Nagel, U. Oertel, P. Friedel, H. Komber, D. Mobius, Langmuir–Blodgett layers from Schiff base copper(II) complexes. *Langmuir* **13**, 4693–4698 (1997)

- M. Pascu, G.J. Clarkson, B.M. Kariuki, M.J. Hannon, Aggregation of imine-based metallo-supramolecular architectures through [small pi]–[small pi] interactions. *Dalton Trans.* **22**, 2635–2642 (2006)
- J.R. Price, Y. Lan, S. Brooker, Pyridazine-bridged copper(I) complexes of bis-bidentate ligands: tetranuclear [2 × 2] grid versus dinuclear side-by-side architectures as a function of ligand substituents. *Dalton Trans.* **18**, 1807–1820 (2007)
- X.H. Zhou, T. Wu, D. Li, Structural variations and spectroscopic properties of copper(I) complexes with bis(schiff base) ligands. *Inorg. Chim. Acta* **359**, 1442–1448 (2006)
- G.Q. Zhang, G.Q. Yang, J.S. Ma, A novel stable CuI complex based on an unconjugated bisanthryl-tethered diimine ligand with tri-coordinate mode. *J. Chem. Crystallogr.* **36**, 631–635 (2006)
- S. Dehghanpour, A. Mahmoudi, R. Hadjikhani, Unusual coordination of tetraphenylborate to silver(I): synthesis and X-ray crystal structure of the complex *N, N'*-bis [3-(2-nitrophenyl) allylidene]ethane-1,2-diamine(tetraphenylborato)silver(I). *J. Braz. Chem. Soc.* **19**, 600–603 (2008)
- A.H. Kianfar, H. Farrokhpour, P. Dehghani, H.R. Khavasi, Experimental and theoretical spectroscopic study and structural determination of nickel(II) tridentate Schiff base complexes. *Spectrochim. Acta Part A* **150**, 220–229 (2015)
- M. Morshedi, M. Amirnasr, A.M.Z. Slawin, J.D. Woollins, A.D. Khalaji, Synthesis and coordination chemistry of new tetradentate N₂S₂ donor Schiff-base ligand ca₂-dapte: mononuclear and dinuclear copper(I) complexes [Cu(ca₂dapte)]ClO₄ and [{Cu(PPh₃)(X)}₂(ca₂dapte)] (X = I and Br). *Polyhedron* **28**, 167–171 (2009)
- S. Das, B.N. Sarkar, K. Bhar, S. Chattopadhyay, H.K. Fun, P. Mitra, B.K. Ghosh, Classical tetradentate chelation and novel bis(bidentate) congregation motifs of a neutral N-donor Schiff base in dinuclear cadmium(II) complexes: synthesis, structure and luminescence behaviour. *Inorg. Chem. Commun.* **13**, 353–357 (2010)
- M. Dolaz, V. McKee, S. Urus, N. Demir, A.E. Sabik, A. Golcu, N. Tumer, Synthesis, structural characterization, catalytic, thermal and electrochemical investigations of bidentate Schiff base ligand and its metal complexes. *Spectrochim. Acta Part A* **76**, 174–181 (2010)
- H. Makio, H. Terao, A. Iwashita, T. Fujita, FI catalysts for olefin polymerization—a comprehensive treatment. *Chem. Rev.* **111**, 2363–2449 (2011)
- G.Y. Nagesh, K. Mahendra Raj, B.H.M. Mruthyunjayaswamy, Synthesis, characterization, thermal study and biological evaluation of Cu(II), Co(II), Ni(II) and Zn(II) complexes of Schiff base ligand containing thiazole moiety. *J. Mol. Struct.* **1079**, 423–432 (2015)
- Y.P. Tian, C.Y. Duan, Z.L. Lu, X.Z. You, Crystal structure and spectroscopic studies on metal complexes containing ns donor ligands derived from *S*-benzylthiocarbamate and *p*-dimethylaminobenzaldehyde. *Polyhedron* **15**, 2263–2271 (1996)
- S. Mandal, G. Rosair, J. Ribas, D. Bandyopadhyay, Synthesis, crystal structure and magnetic characterization of a new phenoxo-bridged binuclear manganese(III) Schiff base complex exhibiting single-molecule-magnet behavior. *Inorg. Chim. Acta* **362**, 2200–2204 (2009)
- J. Welby, L.N. Rusere, J.M. Tanski, L.A. Tyler, Syntheses and crystal structures of mono-, di- and trinuclear cobalt complexes of a salen type ligand. *Inorg. Chim. Acta* **362**, 1405–1411 (2009)
- K. Bernardo, S. Leppard, A. Robert, G. Commenges, F. Dahan, B. Meunier, Synthesis and characterization of new chiral Schiff base complexes with diiminobinaphthyl or diiminocyclohexyl moieties as potential enantioselective epoxidation catalysts. *Inorg. Chem.* **35**, 387–396 (1996)
- V.P. Daniel, B. Murukan, B.S. Kumari, K. Mohanan, Synthesis, spectroscopic characterization, electrochemical behaviour, reactivity and antibacterial activity of some transition metal complexes with 2-(*N*-salicylideneamino)-3-carboxyethyl-4,5-dimethylthiophene. *Spectrochim. Acta Part A* **70**, 403–410 (2008)
- G. Venkatachalam, N. Raja, D. Pandiarajan, R. Ramesh, Binuclear ruthenium(III) Schiff base complexes bearing N₄O₄ donors and their catalytic oxidation of alcohols. *Spectrochim. Acta Part A* **71**, 884–891 (2008)
- T. Yu, K. Zhang, Y. Zhao, C. Yang, H. Zhang, D. Fan, W. Dong, A new trinuclear zinc(II) complex possessing five- and six-coordinated central ions and its photoluminescent property. *Inorg. Chem. Commun.* **10**, 401–403 (2007)
- P. Mukherjee, C. Biswas, M.G.B. Drew, A. Ghosh, Structural variations in Ni(II) complexes of salen type di-Schiff base ligands. *Polyhedron* **26**, 3121–3128 (2007)
- S. Chattopadhyay, G. Boclli, A. Musatti, A. Ghosh, First oxidative synthetic route of a novel, linear mixed valence Co(III)–Co(II)–Co(III) complex with bridging acetate and salen. *Inorg. Chem. Commun.* **9**, 1053–1057 (2006)
- K.C. Gupta, A.K. Sutar, Catalytic activities of Schiff base transition metal complexes. *Coord. Chem. Rev.* **252**, 1420–1450 (2008)
- J.P. Collin, J.P. Sauvage, Electrochemical reduction of carbon dioxide mediated by molecular catalysts. *Coord. Chem. Rev.* **93**, 245–268 (1989)
- C. Amatore, A. Jutand, Activation of carbon dioxide by electron transfer and transition metals. Mechanism of nickel-catalyzed electrocarboxylation of aromatic halides. *J. Am. Chem. Soc.* **113**, 2819–2825 (1991)
- M. Barwiolek, E. Szlyk, A. Surdykowski, A. Wojtczak, New Ni(II) and Cu(II) complexes with unsymmetrical Schiff bases derived from (1*R*,2*R*)(–)-cyclohexanediamine and the application of Cu(II) complexes for hybrid thin layers deposition. *Dalton Trans.* **42**, 11476–11487 (2013)
- P.W. Raess, M.S. Mubarak, M.A. Ischay, M.P. Foley, T.B. Jennermann, K. Raghavachari, D.G. Peters, Catalytic reduction of 1-iodooctane by Ni(I) salen electrogenerated at carbon cathodes in dimethylformamide: effects of added proton donors and a mechanism involving both metal- and ligand-centered one-electron reduction of Ni(II) salen. *J. Electroanal. Chem.* **603**, 124–134 (2007)
- M.P. Foley, P. Du, K.J. Griffith, J.A. Karty, M.S. Mubarak, K. Raghavachari, D.G. Peters, Electrochemistry of substituted salen complexes of Ni(II): Ni(I)-catalyzed reduction of alkyl and acetylenic halides. *J. Electroanal. Chem.* **647**, 194–203 (2010)
- K.S. Alleman, M.J. Samide, D.G. Peters, M.S. Mubarak, J.O.M. Bockris, E.J. Cairns, M. Froment, Z. Galus, Y. Ito, S. Trasatti, T.J. Vander Noot, Catalytic reduction of organohalogen compounds with electrogenerated homogeneous-phase and polymer-bound Co(I) and Ni(I) salen. *Curr. Top. Electrochem.* **6**, 1–31 (1998)
- A.J. Fry, P.F. Fry, Nickel(I) salen-electrocatalyzed reduction of benzal chloride. *J. Org. Chem.* **58**, 3496–3501 (1993)
- D.M. Fang, D.G. Peters, M.S. Mubarak, Catalytic reduction of 6-bromo-1-hexene by Ni(I) salen electrogenerated at glassy carbon cathodes in acetonitrile. *J. Electrochem. Soc.* **148**, E464–E467 (2001)
- P. Vanalabhpatana, D.G. Peters, Catalytic reduction of 1,6-dihaloheptanes by Ni(I) salen electrogenerated at glassy carbon cathodes in dimethylformamide. *J. Electrochem. Soc.* **152**, E222–E229 (2005)
- M.S. Mubarak, W.E. Barker IV, D.G. Peters, Nickel(I) salen-catalyzed reduction of 1-halo-alkyl-2-oxocycloalkancarboxylates: three- and four-carbon ring expansions. *J. Electrochem. Soc.* **154**, F205–F210 (2007)

41. M.C. Burla, R. Caliandro, M. Camalli, B. Carrozzini, G.L. Cascarano, L. De Caro, C. Giacovazzo, G. Polidori, R. Spagna, SIR2004: an improved tool for crystal structure determination and refinement. *J. Appl. Cryst.* **38**, 381–388 (2005)
42. G.M. Sheldrick, A short history of SHELX. *Acta Cryst. A* **64**, 112–122 (2008)
43. L.J. Farrugia, WinGX and ORTEP for windows: an update. *J. Appl. Cryst.* **45**, 849–854 (2012)
44. L.J. Farrugia, ORTEP-3 for windows—a version of ORTEP-III with a graphical user interface (GUI). *J. Appl. Cryst.* **30**, 565 (1997)
45. P.M. Vimal Kumar, P.K. Radhakrishnan, Synthesis, spectral and X-ray structural studies of a NO donor Schiff base ligand and its Ni(II) complexes. *Inorg. Chim. Acta* **375**, 84–92 (2011)
46. S.M. El-Megharbel, A.S. Megahed, M.S. Refat, Preparation, physical and chemical studies on metal complexes of Schiff bases as a nucleus key to prepare nanometer oxides have catalytic applications: nickel (II) complexes derived from 4-aminoantipyrine derivatives. *J. Mol. Liq.* **216**, 608–614 (2016)
47. H. Keypour, M. Shayesteh, M. Rezaeivala, F. Chalabian, L. Valencia, Synthesis and characterization of a series of transition metal complexes with a new symmetrical polyoxaaza macrocyclic Schiff base ligand: X-ray crystal structure of cobalt(II) and nickel(II) complexes and their antibacterial properties. *Spectrochim. Acta Part A* **101**, 59–66 (2013)
48. D. Tomczyk, L. Nowak, W. Bukowski, K. Bester, P. Urbaniak, G. Andrijewski, B. Olejniczak, Reductive and oxidative electrochemical study and spectroscopic properties of nickel(II) complexes with N₂O₂ Schiff bases derived from (±)-*trans*-*N*, *N'*-bis(salicylidene)-1,2-cyclohexanediamine. *Electrochim. Acta* **121**, 64–67 (2014)
49. A. Ghaffari, M. Behzad, M. Pooyan, H.A. Rudbari, G. Bruno, Crystal structures and catalytic performance of three new methoxy substituted salen type nickel(II) Schiff base complexes derived from *meso*-1,2-diphenyl-1,2-ethylenediamine. *J. Mol. Struct.* **1063**, 1–7 (2014)
50. A.D. Khalaji, S.M. Rad, G. Grivani, D. Das, Nickel(II) and copper(II) complexes with an asymmetric bidentate Schiff-base ligand derived from furfurylamine. *J. Therm. Anal. Calorim.* **103**, 747–751 (2011)
51. M. Pooyan, A. Ghaffari, M. Behzad, H.A. Rudbari, G. Bruno, Tetradentate N₂O₂ type Nickel (II) Schiff base complexes derived from *meso*-1, 2-diphenyl-1, 2-ethylenediamine: synthesis, characterization, crystal structures, electrochemistry, and catalytic studies. *J. Coord. Chem.* **66**, 4255–4267 (2013)
52. B. Bouzerafa, A. Ourari, D. Aggoun, R. Ruiz-Rosas, Y. Ouenoughi, E. Morallon, Novel nickel(II) and manganese(III) complexes with bidentate Schiff-base ligand: synthesis, spectral, thermogravimetry, electrochemical and electrocatalytic properties. *Res. Chem. Intermed.* **42**, 4839–4858 (2016)
53. A. Ourari, D. Aggoun, Synthesis and spectral analysis of *N*-substituted pyrrole salicylaldehyde derivatives-electropolymerization of a new nickel(II)-Schiff base complex derived from 6-[3'-*N*-pyrrolpropoxy]-2-hydroxyacetophenone and 1,2-diaminoethane. *J. Iran. Chem. Soc.* **12**, 1893–1904 (2015)
54. A. Ourari, Y. Ouenoughi, D. Aggoun, M.S. Mubarak, E.M. Pasciak, D.G. Peters, Synthesis, characterization, and electrochemical study of a new tetradentate nickel(II)-Schiff base complex derived from ethylenediamine and 5'-(*N*-methyl-*N*-phenylaminomethyl)-20-hydroxyacetophenone. *Polyhedron* **67**, 59–64 (2014)
55. C. Ji, S.E. Day, W.C. Silvers, Catalytic reduction of 1- and 2-bromoethanes by a dinickel(I) Schiff base complex containing two salen units electrogenerated at carbon cathodes in dimethylformamide. *J. Electroanal. Chem.* **622**, 15–21 (2008)